Preprints of the 21st IFAC World Congress (Virtual)
Berlin, Germany, July 12-17, 2020

Control-oriented model reduction for a class of hyperbolic systems with application to managed pressure drilling ⋆

T. C. P. F. Leenen [*,***] **S. Naderi Lordejani** [*] **B. Besselink** [**]
W. H. A. Schilders [***] **N. van de Wouw** [*,****]

[*] *Department of Mechanical Engineering, Eindhoven University of Technology, Eindhoven, The Netherlands (t.c.p.f.leenen@student.tue.nl, s.naderilordejani@tue.nl, n.v.d.wouw@tue.nl)*
[**] *Bernoulli Institute for Mathematics, Computer Science and Artificial Intelligence, University of Groningen, Groningen, The Netherlands (b.besselink@rug.nl)*
[***] *Department of Mathematics and Computer Science, Eindhoven University of Technology, The Netherlands (w.h.a.schilders@tue.nl)*
[****] *Department of Civil, Environmental & Geo-Engineering, University of Minnesota, Minneapolis, USA*

Abstract: This paper presents a model reduction approach for systems of hyperbolic partial differential equations (PDEs) with nonlinear boundary conditions. These systems can be decomposed into a feedback interconnection of a linear hyperbolic subsystem and a static nonlinear mapping. This structure motivates us to reduce the overall model complexity by only reducing the linear subsystem (the PDE part). We show that the linear PDE subsystem can effectively be approximated by a cascaded structure of systems of continuous time difference equations (CTDEs) and ordinary differential equations (ODEs), where the CTDE captures the infinite-dimensional nature of the PDE model. These systems are constructed by adapting an interpolation method based on frequency-domain data. Models in the form of hyperbolic PDEs with nonlinear boundary conditions are for example encountered in managed pressure drilling (MPD). The proposed technique is verified by application to such an MPD model.

Keywords: Model reduction, hyperbolic systems, automatic control, time delay, managed pressure drilling

1. INTRODUCTION

Hyperbolic partial differential equations (PDEs) govern a variety of physical phenomena occurring in fluid mechanics, astrophysics, groundwater flow, meteorology, semiconductors and power systems (Kurganov and Tadmor, 2000). Although hyperbolic models were initially used merely for simulation and analysis purposes, these models have in recent years gained much attention in the design of model-based control systems (Krstic and Smyshlyaev, 2008; Davó et al., 2019). However, system analysis and controller design techniques developed for this type of models are still relatively elementary and those mostly focus on stabilization aspects. Namely, the complexity of these models currently handicaps the design of controllers that can meet more advanced performance criteria.

To enable controller synthesis for such performance criteria, a common approach is to approximate the hyperbolic system by rational models in terms of ordinary differential equations (ODEs) (Litrico and Fromion, 2006; Kaasa et al., 2012; Landet et al., 2013; Naderi Lordejani et al., 2018; Zlotnik et al., 2015), for which systems and control theory is well-developed. A key feature of hyperbolic systems is their advective nature, which causes wave propagation effects (also known as the waterhammer effect in the drilling industry (Kaasa et al., 2012)). As this effect is crucial in many applications, a high-performance controller design should be based on (approximative) models that accurately capture such effects. However, this typically requires high-order approximate ODE models, which in turn hamper the design and implementation of controllers based on such models.

The boundary input-output behavior of hyperbolic systems with a single advection equation can be described exactly by continuous-time difference equations (CTDEs) (Karafyllis and Krstic, 2014). It is also possible to have such exact descriptions for 2×2 hyperbolic systems for special cases of coupling source terms (Cooke and Krumme, 1968). This fact has been known since long and has been used in the delay modeling of lossless transmission lines (see (Răsvan, 2006) for examples). More generally, the presence of coupling source terms leads to delay differential equations with distributed delay terms with complex kernel functions (Auriol and Di Meglio, 2019), which are difficult to handle from both simulation and

⋆ This research has been carried out in the HYDRA project, which has received funding from the European Union's Horizon 2020 research and innovation program under grant agreement No 675731.

system-theoretic perspectives. In this paper, we seek to construct approximate models of low complexity for hyperbolic systems which preserve key system properties, such as the wave propagation effect. Moreover, this approximate model should potentially facilitate the design and implementation of high-performance controllers and also speed up numerical simulations.

In this study, we consider a special class of systems consisting of two sets of linear isothermal Euler equations with coupling source terms and nonlinear boundary conditions. This particular model has strong practical motivations behind it. In particular, it is used to model drilling systems for managed pressure drilling (MPD) applications (Kaasa et al., 2012; Naderi Lordejani et al., 2018).

The contributions of this paper are as follows. First, we show that the original PDE system with nonlinear boundary conditions can be decomposed into a feedback interconnection of a linear distributed-parameter subsystem and a low-dimensional, nonlinear mapping due to the boundary conditions. We care to stress that given the fact that 1) the boundary conditions in the original model have a physical interpretation and 2) the control inputs are applied through the boundary conditions, we are interested in preserving this physical insight in the reduced model. Such structure preservation is supported by the proposed model decomposition. Second, we show that the linear PDE subsystem can effectively be approximated by a series connection of low-order models in terms of CTDEs and ODEs. The CTDE part is employed to embed the advective nature of the system and the ODE part is used to approximate in-domain coupling effects between system variables due to the source terms. Because the wave propagation effect is embedded through the CTDE model, the ODE part no longer needs to be of high-order, as opposed to conventional high-order ODE-based approximate models. Third, we propose an adapted and efficient interpolation technique for the construction of the CTDE and ODE models from frequency-domain data of the original model. Lastly, we apply the proposed model reduction technique to single-phase flow MPD-controlled drilling systems, and present simulation results to illustrate the effectiveness of this method for such MPD applications.

Organization. After introducing notation, a problem statement is given in Section 2. In Section 3, we review the relevance of the proposed model in the context of MPD automation. A model reformulation is presented in Section 4. Section 5 introduces a structure for the reduced model, whereas Section 6 presents a data-based model reduction approach for constructing the reduced model. Numerical examples are provided in Section 7 and conclusions are presented in Section 8.

Notation. $\mathbb{R}$, $\mathbb{C}$ and I_m refer to the fields of real and complex numbers and the $m \times m$ identity matrix, respectively. A block-diagonal matrix with A_1, ..., A_m on the diagonal is represented as $\text{blkdiag}\{A_1, \cdots, A_m\}$.

2. PROBLEM STATEMENT AND MOTIVATIONS

Consider a system of balance laws composed of two sets of linearized isothermal Euler equations (a 2×2 hyperbolic system)

$$\frac{\partial Q}{\partial t} + \Psi_c \frac{\partial Q}{\partial \xi} + F_c Q = 0, \quad Q(0,\xi) = 0, \tag{1}$$

where $\xi \in (0, l)$ and $t > 0$ are the spatial and temporal variables, respectively, and $Q^T(\xi,t) = [q_1^T(\xi,t), q_2^T(\xi,t)]$ is the vector of variables with $q_1^T = [q_{11}, q_{12}]$ and $q_2^T = [q_{21}, q_{22}]$. Note that $q_1(t,\xi), q_2(t,\xi) \in \mathbb{R}^2$. Moreover,

$$\Psi_c = \begin{bmatrix} \Psi & 0 \\ 0 & \Psi \end{bmatrix}, \Psi = \begin{bmatrix} 0 & 1 \\ c^2 & 0 \end{bmatrix}, F_c = \begin{bmatrix} F_1 & 0 \\ 0 & F_2 \end{bmatrix},$$

with c [m/s] and l [m] the speed of sound and length of the spatial domain, respectively. This system is accompanied by nonlinear boundary conditions of the form

$$\Pi_1 \begin{bmatrix} Q(t,0) \\ Q(t,l) \end{bmatrix} - \Pi_2 \psi \left(\Gamma \begin{bmatrix} Q(t,0) \\ Q(t,l) \end{bmatrix}, u(t) \right) = 0, \tag{2}$$

where $u(t) \in \mathbb{R}^p$ is the input vector, $\psi(\cdot,\cdot) \in \mathbb{R}^{n_l}$ is in general a nonlinear function, and $\Pi_1 \in \mathbb{R}^{4\times 8}$, $\Gamma \in \mathbb{R}^{r\times 8}$ and $\Pi_2 \in \mathbb{R}^{4\times n_l}$ are given matrices. Furthermore, we assume that for the matrix $H \in \mathbb{R}^{m\times r}$, the output is given by

$$y(t) = H\Gamma \begin{bmatrix} Q(t,0) \\ Q(t,l) \end{bmatrix}, \tag{3}$$

where we assume that $p \geq m$. Given the system in (1), (2) and (3), the objective is to approximate the input-output behavior of this system from the input u to the output y with a model of a lower complexity which allows for faster yet accurate time-domain simulations. Moreover, this model should possess a structure that potentially facilitates the design of high-performance controllers. Given the fact that the nonlinear boundary conditions have physical interpretation, these equations should be recovered explicitly in the reduced model.

Remark 1. In model in (1), the term F_cQ models the in-domain interactions among the components of Q and it is called the coupling source term.

In the next section, we review the relevance of the presented model in the context of MPD automation.

3. MANAGED PRESSURE DRILLING

Automated MPD is a method for fast and accurate pressure control in drilling to avoid, on the one hand, an influx from underground formations during drilling and, on the other hand, fracturing those formations. For many drilling scenarios, a drilling system with MPD can be described by a linear system of PDEs of the form (1) and boundary conditions of the form (2). Specifically, to model the hydraulics of a drilling system, we use the so-called U-tube modeling approach, where the drilling system is modeled as two connected pipes which respectively model the drillstring and annulus of the drilling system. The flow behavior in each of these pipes is then modeled by a set of Euler equations (Strecker et al., 2017; Kaasa et al., 2012), leading to a PDE model of the form (1). For a drilling system, l represents the length of the well, c is the sound velocity in the drilling mud and F_c is characterized by

$$F_1 = \begin{bmatrix} 0 & 0 \\ -g\sin(\theta) & \dfrac{32\mu}{\rho_0 d_{\text{d}}^2} \end{bmatrix}, F_2 = \begin{bmatrix} 0 & 0 \\ g\sin(\theta) & \dfrac{32\mu}{\rho_0 d_{\text{a}}^2} \end{bmatrix},$$

with θ [rad] , μ [Pa.s], d_{a} [m], d_{d} [m] and g [m/s^2] being the well inclination, viscosity of mud, hydraulic diameter of the annulus, inner diameter of the drillstring and

gravitational acceleration, respectively. With this selection of parameters, q_1 represents the vector of the density and momentum along the drillstring, i.e., $q_{11} = \rho_{\mathrm{d}}$ [kg/m^3] and $q_{12} = \rho_{\mathrm{d}} v_{\mathrm{d}}$ [kg/(m^{2}s)], with v_{d} [m/s] the speed of liquid in the drillstring. Likewise, q_2 is composed of the density and momentum of the drilling mud along the annulus. The boundary conditions of this system given by the pump, bit, mass conservation over the bit and choke equations, are as follows:

$$\begin{aligned} A_{\mathrm{d}}(0)q_{12}(t,0) - J_{\mathrm{p}}(t) &= 0,\\ A_{\mathrm{d}}(l)q_{12}(t,l) - A_{\mathrm{nz}}c_d c\sqrt{2q_{11}(t,l)(q_{11}(t,l)-q_{21}(t,0))} &= 0,\\ A_{\mathrm{d}}(l)q_{12}(t,l) - A_{\mathrm{a}}(0)q_{22}(t,0) &= 0,\\ A_{\mathrm{a}}(l)q_{22}(t,l) - k_{\mathrm{c}}cG(z_{\mathrm{c}}(t))\sqrt{2q_{21}(t,l)(q_{21}(t,l)-\rho_0)} &= 0, \end{aligned} \tag{4}$$

where A_{d} [m^2], A_{a} [m^2], A_{nz} [m^2], c_d [-] and k_{c} [m^2] are the area of the drillstring, area of the annulus, area of the bit nozzles, discharge coefficient of the bit nozzles and the flow factor of the choke, respectively. Furthermore, J_{p} [kg/s], z_{c} [-] and $G(\cdot)$ are the pump mass flow rate, the choke opening an the choke characteristic. In MPD, the main control inputs are J_{p} and z_{c}. For details, see (Naderi Lordejani et al., 2020, 2018; Naderi Lordejani et al., 2020).

4. MODEL REFORMULATION

To be able to reduce the complexity of the model described in (1) and (2) while preserving the structure of the boundary conditions, we decompose the model into a feedback interconnection of a linear subsystem and a nonlinear mapping. This decomposition is motivated by the fact that the nonlinearities occur in the model only locally, and it enables us to reduce the complexity of this model by only reducing the complexity of the linear PDE part and leaving the nonlinearities untouched. The next statement presents the details of the decomposed model.

Statement 1. Consider the system described by (1), (2) and (3). This system can be cast into a feedback interconnection of an infinite-dimensional linear system Σ and a nonlinear mapping $\psi(\cdot,\cdot)$ of the following forms:

$$\Sigma : \begin{cases} \dfrac{\partial Q}{\partial t} + \Psi_c \dfrac{\partial Q}{\partial \xi} + F_c Q = 0,\ Q(\xi,0) = 0,\\ \Pi_1 \begin{bmatrix} Q(t,0)\\ Q(t,l)\end{bmatrix} = \Pi_2 v(t),\\ w(t) = \Gamma \begin{bmatrix} Q(t,0)\\ Q(t,l)\end{bmatrix},\ y(t) = Hw(t), \end{cases} \tag{5}$$

$$v(t) = \psi(w(t), u(t)), \tag{6}$$

where $w(t) \in \mathbb{R}^r$ is the output of Σ and $v(t) \in \mathbb{R}^{n_l}$ is its input.

A block diagram of the reformulated model is presented in Fig. 1. Considering this figure, the model complexity reduction objective in this paper is pursued by approximating Σ by a model $\hat{\Sigma}$ of desirable properties, which are yet to be introduced.

Remark 2. We assume that the linear system Σ is exponentially stable for zero input, i.e., there exist $a > 0$ and $b > 0$ such that

$$\sqrt{\int_0^l Q^T(t,s)Q(t,s)\,ds} \le ae^{-bt}\sqrt{\int_0^l Q^T(0,s)Q(0,s)\,ds},$$

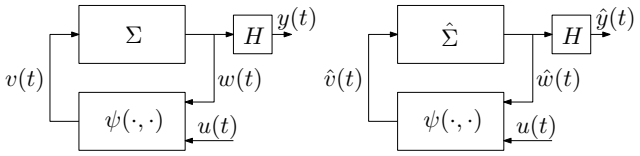

Fig. 1. A block diagram of the reformulated model in Statement 1: (left) before reduction, (right) after reduction.

for all initial conditions $Q(0,\cdot) \in \mathcal{L}_2([0,l],\mathbb{R}^4)$ and zero input $v = 0$.

The next lemma gives the transfer function of Σ.

Lemma 3. Consider the linear system Σ in (5). The matrix transfer function $T(s)$ of this system from the input v to the output w in the Laplace domain is given by

$$T(s) = \Gamma \begin{bmatrix} I_4\\ e^{\Xi(s)l}\end{bmatrix} \left(\Pi_1 \begin{bmatrix} I_4\\ e^{\Xi(s)l}\end{bmatrix}\right)^{-1} \Pi_2, \tag{7}$$

where $s \in \mathbb{C}$ is the Laplace variable and $\Xi(s) = \mathrm{blkdiag}(\Xi_1, \Xi_2)$, $\Xi_i(s) = -\Psi^{-1}(sI_2 + F_i)$, for $i = 1, 2$, and $\exp(\Xi\xi) = \mathrm{blkdiag}(\exp(\Xi_1\xi), \exp(\Xi_2\xi))$.

Proof. The proof has been omitted for the sake of brevity.

Remark 4. The explicit expression of $\exp(\Xi_i(s)\xi)$, $i = 1, 2$, in Lemma 3 is given by

$$e^{\Xi_i(s)\xi} = e^{-\alpha\xi} \begin{bmatrix} m_{11}(s,\xi) & -\dfrac{s+f_{22}}{c^2\beta}\sinh(\beta\xi)\\ -\dfrac{s+f_{11}}{\beta}\sinh(\beta\xi) & m_{22}(s,\xi)\end{bmatrix}, \tag{8}$$

with

$$m_{11}(s,\xi) = \cosh(\beta(s)\xi) + \left(\alpha - \frac{f_{21}}{c^2}\right)\frac{\sinh(\beta(s)\xi)}{\beta(s)}, \tag{9}$$

$$m_{22}(s,\xi) = \cosh(\beta(s)\xi) + (\alpha - f_{12})\frac{\sinh(\beta(s)\xi)}{\beta(s)}, \tag{10}$$

and $\beta(s) = \sqrt{\alpha^2 + (s+f_{22})(s+f_{11})/c^2 - f_{12}f_{21}/c^2}$ and $\alpha = 0.5(f_{12} + f_{21}/c^2)$, for

$$F_i = \begin{bmatrix} f_{11} & f_{12}\\ f_{21} & f_{22}\end{bmatrix},$$

where the subscript i has been dropped from the elements of F_i for simplicity.

5. STRUCTURE OF THE REDUCED MODEL

As the first step in designing the approximate model $\hat{\Sigma}$, we design a structure for it in this section.

If we neglect the source term in (5), i.e., if we assume $F_c = 0$, the model reduces to a number of pure advection equations with the boundary conditions in (2). It is well-known that an advection equation is a representation for a delay of l/c seconds. It means that Σ in the absence of source terms can be modeled by a system of CTDEs, which represent the transport phenomena in the system. However, the source terms lead to distributed in-domain couplings among the traveling waves. Our observations show that these interactions in particular affect the low-frequency behavior of the system Σ. We can also show that $\exp(\Xi_i(s)l)$, $i = 1, 2$, in (7) converges to a periodic behavior of a period of $2\pi c/l$ at high frequencies. A Bode plot of the function $\exp(\Xi_1(j\omega)l)$ for the drillstring of a

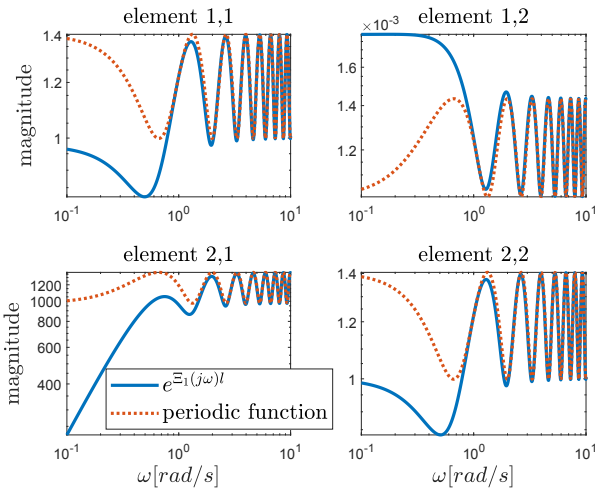

Fig. 2. Element-wise comparison of $\exp(\Xi_1(j\omega)l)$ and the periodic function to which it converges for $\omega \to \infty$, for the drillstring of a drilling system with parameter values in Table 1, except for the viscosity which is set to be $\mu = 0.35$ Pa.s.

drilling system is plotted in Fig. 2. This figure illustrates the fact that $\exp(\Xi_1(j\omega)l)$ converges to a periodic function when $\omega \to \infty$. The periodic behaviour of $\exp(\Xi_i(j\omega)l)$, which is also induced in $T(j\omega)$, is a manifestation of the advective nature of the system. Thus, we conclude that in the presence of these source terms, the system behaviour is composed of two dominating aspects: 1) advection and 2) dynamics governing the shape of advective waves at the boundaries. As said before, the (advection-induced) transport aspects can be modeled by CTDEs. This is the dominating aspect at high frequencies. Given that the second aspect has its most dominance at low frequencies, we compensate for that by a system of ODEs.

This explanation motivates us to consider for $\hat{\Sigma}$ a structure which consists of an interconnection of a CTDE model Σ_{ctde} and an ODE model Σ_{ode}. Here, we adapt a series interconnection between Σ_{ctde} and Σ_{ode}, as in Fig. 3, and refer to it as the cascaded system. We propose the following realizations for Σ_{ctde} and Σ_{ode}

$$\Sigma_{\text{ctde}}: \begin{cases} E_1 x_1(t) = -A_1 x_1(t-\tau) + B_1 \hat{v}(t), \\ z(t) = C_1 x_1(t), \end{cases} \tag{11}$$

$$\Sigma_{\text{ode}}: \begin{cases} E_2 \dot{x}_2(t) = A_2 x_2(t) + B_2 z(t), \\ \hat{w}(t) = C_2 x_2(t) + D_2 z(t), \end{cases} \tag{12}$$

where $x_1(t) \in \mathbb{R}^{n_1}$ and $x_2(t) \in \mathbb{R}^{n_2}$ are the state vectors, $z(t) \in \mathbb{R}^m$ is the output of Σ_{ctde} and the input of Σ_{ode}. Moreover, τ is the delay and E_1, E_2, A_1, A_2, C_1, C_2, B_1, B_2 and D_2 are system matrices of appropriate dimensions which, together with the orders n_1 and n_2, will be constructed in the next section.

Remark 5. The transfer function $T_{\text{ctde}}(j\omega)$ of the CTDE is a periodic function with a period of $2\pi/\tau$, and this function should capture the periodic behavior of $T(j\omega)$, the transfer function of Σ, at high frequencies. Thus, given $2\pi c/l$, the period of $T(j\omega)$, we should set $\tau = l/c$.

Remark 6. Here, we have assumed a series interconnection between Σ_{ctde} and Σ_{ode} because we are interested in interconnections that are more suitable for controller synthesis and system analyses, such as stability analysis.

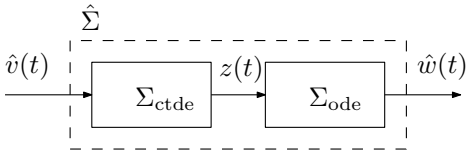

Fig. 3. A block diagram of the proposed cascaded structure for $\hat{\Sigma}$.

Remark 7. For the series interconnection in Fig. 3, we regard $z(t)$ as an approximation of the output $\hat{w}(t)$, which will be refined by Σ_{ode}. Therefore, the dimension of $z(t)$ is chosen to equal that of $\hat{w}(t)$.

The next section discusses the construction of Σ_{ode} and Σ_{ctde} to obtain an accurate approximation for Σ.

6. DATA-BASED MODEL ORDER REDUCTION

In this section, we introduce a method that is able to construct a general class of systems based on an input-output description of the system in the Laplace domain. This method is mainly based on (Schulze et al., 2018) and (Schulze and Unger, 2016) and it can be applied to a class of systems that can be represented by a transfer function of the form

$$\hat{T}(s) = CK^{-1}(s)B, \tag{13}$$

where $C \in \mathbb{R}^{m\times n}$, $B \in \mathbb{R}^{n\times p}$, and $K(s)$ has a general structure of the form $K(s) = \sum_{k=1}^{N} h_k(s)A_k$. Here, $\{h_1(s), ..., h_N(s)\}$ is a linearly independent set of functions such that $h_k(s) : \mathbb{C} \to \mathbb{C}$ is meromorphic for $k = 1, ..., N$ (Schulze et al., 2018). The structured transfer function (13) represents a large class of systems. For example, the transfer function of a CTDE system (as for (11)) can be written in this form by taking $h_1(s) = 1$ and $h_2(s) = \exp(-\tau s)$, and a first-order ODE structure (as for 12) by $h_1(s) = s$ and $h_2(s) = -1$, both for $N = 2$. The data-driven method proposed in (Schulze et al., 2018) supports constructing (approximate) system models with a transfer function of the form (13) that satisfy certain interpolation conditions. To use this method, we first define which data of the to-be-approximated transfer function $T(s)$ by $\hat{T}(s)$ is available. This data is obtained by evaluating $T(s)$ at certain (interpolation) points in the complex plane. We assume that the data sets $\{\lambda_i, r_i, w_i, \mu_i, l_i, v_i\}_{i=1}^{n}$, that satisfy

$$T(\lambda_i)r_i = w_i, \quad l_i^T T(\mu_i) = v_i^T, \ i = 1, 2, ..., n, \tag{14}$$

are given. Here, n is the number of the interpolation points, λ_i, $\mu_i \in \mathbb{C}$ are the interpolation points, $r_i \in \mathbb{C}^p$, $l_i \in \mathbb{C}^m$ are the right and left tangential direction vectors and $w_i \in \mathbb{C}^m$, $v_i \in \mathbb{C}^p$ are the corresponding system responses. The data λ_i and μ_i and directions r_i and l_i can be chosen arbitrarily provided $T(s)$ exists at these points.

The approach by Schulze et al. (2018) enables us to construct a realization (13), such that its transfer function satisfies the interpolation conditions

$$\hat{T}(\lambda_i)r_i = T(\lambda_i)r_i = w_i, \tag{15}$$

$$l_i^T \hat{T}(\mu_i) = l_i^T T(\mu_i) = v_i^T, \tag{16}$$

for all $i = 1, 2, ..., n$. For convenience, we collect the interpolation data in a matrix form as follows:

$$\begin{aligned} &\Lambda := \text{diag}(\lambda_1, ..., \lambda_n), \ M := \text{diag}(\mu_1, ..., \mu_n), \\ &R := [r_1, ..., r_n], \ L := [l_1, ..., l_n], \\ &W := [w_1, ..., w_n], \ V := [v_1, ..., v_n]. \end{aligned} \tag{17}$$

Next, we present theorems which allow for the construction of realizations for Σ_{ctde} and Σ_{ode} from the interpolation data. The CTDE Σ_{ctde} part of the reduced cascaded realization $\hat{\Sigma}$ can be constructed using following result.

Theorem 8. Let $\{\lambda_i\}_{i=1}^n \cap \{\mu_i\}_{i=1}^n = \emptyset$, and suppose that $T(s)$ exists for every $s \in \{\lambda_i\}_{i=1}^n \cup \{\mu_i\}_{i=1}^n$. Moreover, let (E_1, A_1, B_1, C_1) be given by

$$\begin{aligned}
[E_1]_{i,j} &= \frac{e^{-\tau\mu_i} v_i^T r_j - l_i^T w_j e^{-\tau\lambda_j}}{e^{-\tau\mu_i} - e^{-\tau\lambda_j}},\ i,j = 1,...,n,\\
[A_1]_{i,j} &= \frac{v_i^T r_j - l_i^T w_j}{e^{-\tau\lambda_j} - e^{-\tau\mu_i}},\ i,j = 1,...,n,\\
B_1 &= V^T,\ C_1 = W.
\end{aligned} \tag{18}$$

Then the realization Σ_{ctde} given by (11) with the corresponding transfer function

$$T_{\text{ctde}}(s) = C_1 \left(E_1 + e^{-\tau s} A_1\right)^{-1} B_1,$$

satisfies the interpolation conditions in (15) and (16).

Proof. This theorem presents a special case of results in (Schulze et al., 2018), where a detailed proof can be found.

Similarly, the result in the next theorem allows for the construction of the ODE part of the cascaded system.

Theorem 9. Let $\lambda_i \neq \mu_j$ for all $i,j = 1,...,n$, and suppose that $T(s)$ exists for every $s \in \{\lambda_i\}_{i=1}^n \cup \{\mu_i\}_{i=1}^n$. Moreover, let (E_2, A_2, B_2, C_2) be given by

$$\begin{aligned}
[E_2]_{i,j} &= \frac{l_i^T w_j - v_i^T r_j}{\mu_i - \lambda_j},\ i,j = 1,..,n,\\
[A_2]_{i,j} &= \frac{\mu_i v_i^T r_j - l_i^T w_j \lambda_j}{\lambda_j - \mu_i} + l_i^T D_2 r_j,\ i,j = 1,...,n,\\
B_2 &= V^T - D_2 R,\ C_2 = W - L^T D_2,
\end{aligned} \tag{19}$$

for a given $D_2 \in \mathbb{R}^{m\times p}$. Then, the realization of Σ_{ode} given by (12) with corresponding transfer function

$$T_{\text{ode}}(s) = C_2 \left(sE_2 - A_2\right)^{-1} B_2 + D_2,$$

satisfies the interpolation conditions in (15) and (16).

Proof. This theorem presents a specific case of results in (Schulze et al., 2018), where a detailed proof can be found.

Remark 10. The data matrices M, Λ, V, W, L, R and the order n in Theorem 8 are not the same as those in Theorem 9, although this may seem to be the case due to abuse of notation here. We use two distinct data sets. In particular, M^1, Λ^1, V^1, W^1, L^1, R^1 and n_1 will denote the interpolation data that are used for the CTDE part, and M^2, Λ^2, V^2, W^2, L^2, R^2 and n_2 contain the interpolation data used for the construction of Σ_{ode} using Theorem 9.

The procedure of constructing the reduced model depicted in Fig. 3 is detailed in Algorithm 1. In this algorithm, we first construct a realization for Σ_{ctde} from transfer function data of the original PDE model, while choosing the interpolation points in the high-frequency range as the PDE dynamics is well approximated by the CTDE in that range, see Section 5. Next, we construct Σ_{ode} in such a way that it compensates for the approximation error between $T(s)$ and $T_{\text{ctde}}(s)$ in the low-frequency range.

Remark 11. The feedthrough matrix D_2 in Theorem 9 is set to I_r in Algorithm 1. This enables to achieve the objective of $T(j\omega) \to T_{\text{ctde}}(j\omega)$ for $\omega \to \infty$ following $T_{\text{ode}}(j\omega) \to D_2$ for $\omega \to \infty$.

Algorithm 1: Construction of Σ_{ctde} and Σ_{ode}

Input: M^1, Λ^1, V^1, W^1, L^1, R^1, M^2, Λ^2, L^2, R^2 and $T(s)$ in (7)

Output: Realizations (E_1, A_1, B_1, C_1) and $(E_2, A_2, B_2, C_2, D_2)$ for Σ_{ctde} and Σ_{ode}

1 Construct (E_1, A_1, B_1, C_1) and $T_{\text{ctde}}(s)$ from M^1, Λ^1, V^1, W^1, L^1 and R^1 using Theorem 8.

2 For $T(s)$ as in (7), compute the error transfer function

$$T_{\text{e}}(s) := T(s)T_{\text{ctde}}^T(s)\left(T_{\text{ctde}}(s)T_{\text{ctde}}^T(s)\right)^{-1}.$$

3 Compute W^2 and V^2 based on $T_{\text{e}}(s)$ from M^2, Λ^2, R^2 and L^2.

4 Set $D_2 = I_r$.

5 Construct(E_2, A_2, B_2, C_2) and $T_{\text{ode}}(s)$ using Theorem 9 by interpolating $T_{\text{e}}(s)$ for M^2, Λ^2, V^2, W^2, L^2, R^2.

Table 1. Parameters of the drilling system.

Parameter	Value	Parameter	Value
d_{a}	0.0953 [m]	A_{a}	0.02613[m^2]
d_{d}	0.1088[m]	A_{d}	0.0093 [m^2]
l	2320 [m]	θ	1.4455 [rad]
c	980 [m/s]	g	9.81 [m/s^2]
A_{nz}	5.77$\times$ 10^{-4}[m^2]	c_d	0.8 [-]
ρ_0	1260 [kg/m^3]	μ	0.035 [Pa$\cdot$ s]
k_{c}	0.002 [m^2]		

7. NUMERICAL ILLUSTRATIONS

In this section, we apply the presented model reduction technique to an MPD hydraulics model with its nonlinear boundary conditions as discussed in Section 3. The parameter values of the model are reported in Table 1.

We obtain the matrices Π_1 and Π_2 in (2) by linearizing the boundary conditions around an operating equilibrium. In this example $w^T(t) = [\tilde{\rho}_{\text{d}}(t,l), \tilde{\rho}_{\text{a}}(t,0), \tilde{\rho}_{\text{a}}(t,l)]$, as in (5), contains the perturbed mud density at the bottom of the well in both drillstring and annulus and at the choke. We also take $y = w$, i.e., $H = I_3$. The input $u^T = [\tilde{J}_{\text{p}}, \tilde{z}_{\text{c}}]$ contains the perturbed pump flow rate and the perturbed choke opening. The interpolation points for $n_1, n_2 = 6$ are taken as $\lambda_2 = \lambda_1^*$, $\lambda_4 = \lambda_3^*$, $\lambda_6 = \lambda_5^*$ and $\mu_2 = \mu_1^*$, $\mu_4 = \mu_3^*$, $\mu_6 = \mu_5^*$, and the interpolation directions are taken as unit vectors of appropriate dimensions.

We first compare the approximate and original models in frequency domain, while ignoring the nonlinear boundary conditions, by comparing the transfer function $T(s)$ of Σ to that $\hat{T}(s)$ of the approximate cascaded system $\hat{\Sigma}$. Results of this comparison are shown in Fig. 4, where we can observe the high accuracy of $\hat{T}(j\omega)$ in approximating $T(j\omega)$. Next, we compare the total nonlinear model of the MPD process with its (nonlinear) approximate version in time domain. To numerically implement the nonlinear PDE model, we have used the Kurganov-Tadmor (KT) scheme (Kurganov and Tadmor, 2000) with 1000 cells. Fig. 5 shows the response of the downhole pressure in the annulus to a step signal in the choke and pump for the original PDE model and the approximate model. As can be observed, the nonlinear cascaded approximation yields an accurate approximation of the original system response.

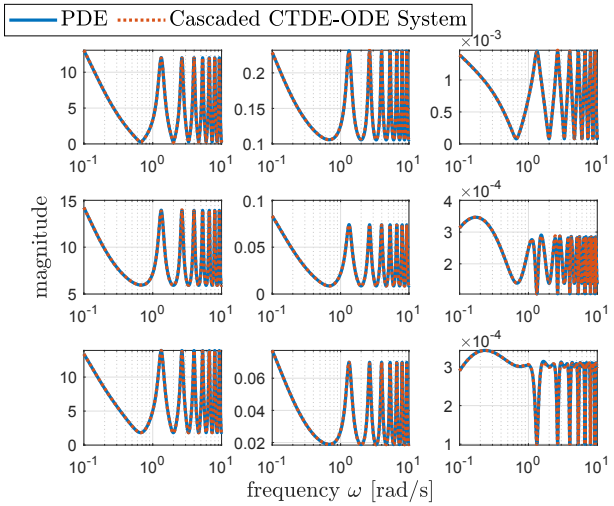

Fig. 4. Element-wise comparison between the magnitude of frequency response function of Σ (PDE) and that of $\hat{\Sigma}$ (approximate cascaded system) in the MIMO example.

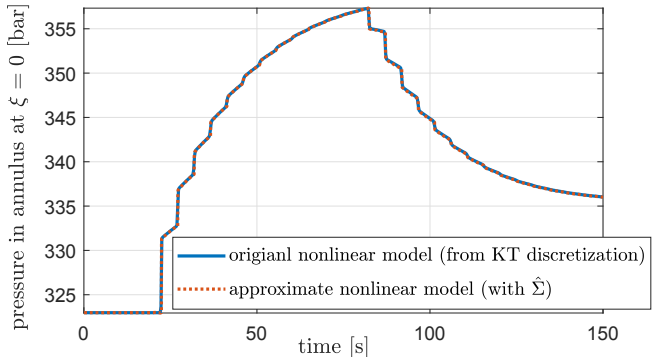

Fig. 5. Comparison between the time-domain response of the reduced nonlinear model and the original model obtained using a KT-discretization. The input is a step of -0.1 in the choke opening $\tilde{z}_c(t)$ at $t = 20$ s and a step of 10 kg/(m^{3}s) in the pump flow $\tilde{J}_p(t)$ at $t = 80$ s. The output is the downhole pressure.

8. CONCLUSIONS

In this paper, a new model structure is introduced to approximate a class of hyperbolic partial differential equations with nonlinear boundary conditions. This structure is composed of a cascaded interconnection of a continuous time delay equation and a system of ordinary differential equations. The aim of this approximation is to obtain low-order input-output models which facilitate control design and enable fast model-based simulations. The cascaded interconnection introduced in this paper is able to accurately capture the infinite-dimensional behaviour of the considered PDE models. In particular, numerical examples show that the approximation method introduced here is able to accurately model managed pressure drilling scenarios. Prospective directions for future work are 1) to use the reduced model for the design of pressure control systems for managed pressure drilling and 2) to generalize the proposed model reduction approach to other classes of PDE systems.

REFERENCES

Auriol, J. and Di Meglio, F. (2019). An explicit mapping from linear first order hyperbolic PDEs to difference systems. *Systems & Control Letters*, 123, 144–150.

Cooke, K.L. and Krumme, D.W. (1968). Differential-difference equations and nonlinear initial-boundary value problems for linear hyperbolic partial differential equations. *J. Math. Anal. Appl.*, 24(2), 372 – 387.

Davó, M.A., Bresch-Pietri, D., Prieur, C., and Di Meglio, F. (2019). Stability analysis of a 2×2 linear hyperbolic system with a sampled-data controller via backstepping method and looped-functionals. *IEEE Trans. Automatic Control*, 64(4), 1718–1725.

Kaasa, G.O., Stamnes, Ø.N., Aamo, O.M., and Imsland, L.S. (2012). Simplified hydraulics model used for intelligent estimation of downhole pressure for a managed-pressure-drilling control system. *SPE Drilling & Completion*, 27(01), 127–138.

Karafyllis, I. and Krstic, M. (2014). On the relation of delay equations to first-order hyperbolic partial differential equations. *ESAIM: Control, Optimisation and Calculus of Variations*, 20(3), 894–923.

Krstic, M. and Smyshlyaev, A. (2008). *Boundary Control of PDEs*. Advances in Design and Control. Society for Industrial and Applied Mathematics.

Kurganov, A. and Tadmor, E. (2000). New high-resolution central schemes for nonlinear conservation laws and convection-diffusion equations. *Journal of Computational Physics*, 160(1), 241–282.

Landet, I.S., Pavlov, A., and Aamo, O.M. (2013). Modeling and control of heave-induced pressure fluctuations in managed pressure drilling. *IEEE Trans. Control Systems Technology*, 21(4), 1340–1351.

Litrico, X. and Fromion, V. (2006). $\mathcal{H}_\infty$ control of an irrigation canal pool with a mixed control politics. *IEEE Trans. Control Systems Technology*, 14(1), 99–111.

Naderi Lordejani, S., Abbasi, M.H., and et al. (2020). Modeling and numerical implementation of managed pressure drilling systems for the assessment of pressure control systems. *SPE Drilling & Completion*, Accepted.

Naderi Lordejani, S., Besselink, B., Abbasi, M.H., Kaasa, G.O., Schilders, W.H.A., and van de Wouw, N. (2018). Model order reduction for managed pressure drilling systems based on a model with local nonlinearities. In *Proceeding of the 3rd IFAC workshop on Automatic Control in Offshore Oil and Gas Production*. Denmark.

Naderi Lordejani, S., Besselink, B., Abbasi, M.H., Kaasa, G.O., Schilders, W.H.A., and van de Wouw, N. (2020). Control-oriented modelling for managed pressure drilling automation using model order reduction. *IEEE Trans. Control Systems Technology*, Accepted.

Răsvan, V. (2006). Functional differential equations of lossless propagation and almost linear behavior. *IFAC Proceedings Volumes*, 39(10), 138–150.

Schulze, P. and Unger, B. (2016). Data-driven interpolation of dynamical systems with delay. *Systems and Control Letters*, 97, 125 – 131.

Schulze, P., Unger, B., Beattie, C., and Gugercin, S. (2018). Data-driven structured realization. *Linear Algebra and its Applications*, 537, 250 – 286.

Strecker, T., Aamo, O.M., and Manum, H. (2017). Simulation of heave-induced pressure oscillations in Herschel-Bulkley muds. *SPE Journal*, 22(05), 1635–1653.

Zlotnik, A., Dyachenko, S., Backhaus, S., and Chertkov, M. (2015). Model reduction and optimization of natural gas pipeline dynamics. In *ASME Dynamic Systems and Control Conference*. Columbus, Ohio, USA.